

Solubility and Decomposition Kinetics of Nitrous Acid in Aqueous Solution

Jong-Yoon Park[†] and Yin-Nan Lee*

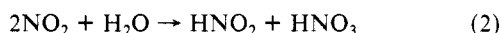
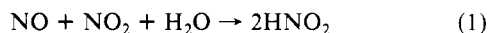
Environmental Chemistry Division, Department of Applied Science, Brookhaven National Laboratory, Upton, New York 11973 (Received: March 12, 1988)

The Henry's law solubility and the decomposition reaction kinetics of nitrous acid (HNO₂) in aqueous solutions have been determined by measuring the material distribution between the gas and liquid phase of the pertinent species with the use of a bubbler-type gas-liquid reactor in conjunction with a high-sensitivity chemiluminescence NO_x detector. The pH-dependent solubility of N(III) (≡HNO₂ + NO₂⁻) was measured for the pH range 2.13-3.33. The Henry's law coefficient and the acid dissociation constant of HNO₂ corresponding to 25 °C are determined to be 49 ± 3 M atm⁻¹ and (5.3 ± 0.4) × 10⁻⁴ M, respectively. The temperature dependence of the solubility over the range 0-30 °C yielded ΔH^o_{sol} = -9.7 ± 0.3 kcal mol⁻¹ and ΔS^o_{sol} = -24.8 ± 0.7 cal mol⁻¹ K⁻¹. The rate constants of the aqueous-phase reactions 2HNO₂ ⇌ NO + NO₂ + H₂O (5) and 2NO₂ + H₂O → H⁺ + NO₃⁻ + HNO₂ (6) determined at 22.0 ± 0.1 °C are k₅ = 13.4 ± 1.0, k₋₅ = (1.6 ± 0.1) × 10⁸, and k₆ = (8.4 ± 1.5) × 10⁷, all in units of M⁻¹ s⁻¹. The values of ΔG^o_{sol} and ΔS^o_{sol} for the dissolution of HNO₂ determined in this work are at variance with the latest values recommended by the National Bureau of Standards but are essentially identical with the previously selected set of values. The rather limited solubility of HNO₂, in combination with its low atmospheric concentrations, suggests that HNO₂ by itself contributes insignificantly to the acidification of atmospheric water, e.g., cloudwater. However, aqueous-phase reactions that produce HNO₂ followed by degassing remain a plausible route for the production of atmospheric HNO₂.

Introduction

The chemistry of nitrogen oxides in the atmosphere is important not only because these species ultimately form nitric acid that contributes much of the strong acid deposited to the earth surface but also because they play pivotal roles in the formation of secondary photooxidants, such as ozone, hydroxyl radical, and hydrogen peroxide, that in turn control in a major way the oxidation of sulfur dioxide and other atmospheric species such as hydrocarbons.^{1,2} Consequently, a systematic characterization of the chemistry of the nitrogen species is necessary to gain a full understanding of the overall role that it plays in atmospheric chemistry.

Among the various nitrogen species, nitrous acid (HNO₂) is considered one of the less well understood ones. For example, although the nighttime buildup of gaseous HNO₂ has been indicated by a number of reports³⁻⁶ and a concentration as high as 8 ppb has been observed,⁴ the mechanism by which this species is produced remains highly uncertain.^{7,8} Since nitrous acid in the atmosphere is thought to be important in providing early morning hydroxyl radical, which would initiate photochemical reactions,^{9,10} identification of the pathways for its formation has been the subject of much research.¹¹⁻¹⁴ Nitrous acid further serves as an acidifying agent of atmospheric water, and as an interferent in the measurement of HNO₃ by a NO_x chemiluminescence detector.¹⁵ Since one potentially important route for the formation of HNO₂ may be the reactions of NO_x (≡NO + NO₂) with liquid water, i.e.



followed by the liberation of this compound from aqueous solution to the gas phase, it is necessary to determine the aqueous-phase solubility and stability of HNO₂ to evaluate the importance of such a pathway.

The reactions of nitrogen oxides in aqueous solution have been widely studied because of their importance in the industrial manufacturing of nitric acid¹⁶ and in the emission control of these species.¹⁷⁻²⁰ In addition, the reactive dissolution reactions, i.e., physical dissolution followed by chemical reactions in aqueous solution, have been carefully examined because they may be responsible for the transformation and removal of atmospheric nitrogen oxides via the so-called "wet scavenging" process. These reactions have been suggested to play important roles not only

in the production of nitrogen oxyacids, which contribute to acid precipitation, but also in the atmospheric residence time of these species.²¹⁻²⁵ Since the overall rates of these absorption processes are found to be governed by the physical solubilities of the nitrogen oxides involved and the concomitant reaction kinetics in aqueous solutions, these quantities must be determined to evaluate the contributions that the gas-aqueous reactions make to atmospheric chemistry and to industrial processes.

(1) Seinfeld, J. H. *Atmospheric Chemistry and Physics of Air Pollution*; Wiley: New York, 1986; pp 118-134.

(2) Finlayson-Pitts, B. J.; Pitts, J. N., Jr. *Atmospheric Chemistry: Fundamentals and Experimental Techniques*; Wiley: New York, 1986.

(3) Perner, D.; Platt, U. *Geophys. Res. Lett.* **1979**, *6*, 917.

(4) Harris, G. W.; Carter, W. P. L.; Winer, A. M.; Pitts, J. N., Jr.; Platt, U.; Perner, D. *Environ. Sci. Technol.* **1982**, *16*, 414.

(5) Pitts, J. N., Jr.; Biermann, H. W.; Atkinson, R.; Winer, A. M. *Geophys. Res. Lett.* **1984**, *11*, 557.

(6) Sjödin, A.; Ferm, M. *Atmos. Environ.* **1985**, *19*, 985.

(7) Stockwell, W. R.; Calvert, J. C. *J. Geophys. Res.* **1983**, *88*, 6673.

(8) Atkinson, R.; Carter, W. P. L.; Pitts, J. N., Jr.; Winer, A. M. *Atmos. Environ.* **1986**, *20*, 408.

(9) Cox, R. A.; Derwent, R. G. *J. Photochem.* **1977**, *6*, 23.

(10) Stockwell, W. R.; Calvert, J. G. *J. Photochem.* **1978**, *8*, 193.

(11) Sakamaki, F.; Hatakeyama, S.; Akimoto, H. *Int. J. Chem. Kinet.* **1983**, *15*, 1013.

(12) Pitts, J. N., Jr.; Sanhueza, E.; Atkinson, R.; Carter, W. P. L.; Winer, A. M.; Harris, G. W.; Plum, C. N. *Int. J. Chem. Kinet.* **1984**, *16*, 919.

(13) Akimoto, H.; Takagi, H.; Sakamaki, F. *Int. J. Chem. Kinet.* **1987**, *19*, 539.

(14) Svensson, R.; Ljungström, E.; Lindqvist, O. *Atmos. Environ.* **1987**, *21*, 1529.

(15) Sanhueza, E.; Plum, C. N.; Pitts, J. N., Jr. *Atmos. Environ.* **1984**, *18*, 1029.

(16) Chilton, T. H. *Strong Water*; M.I.T. Press: Cambridge, MA, 1968.

(17) Hoftyzer, P. J.; Kwanten, F. J. G. In *Gas Purification Processes for Air Pollution Control*; Nonhebel, G., Ed.; Newnes-Butterworths: London, 1972; Chapter 5, Part B.

(18) Sherwood, T. K.; Pigford, R. L.; Wilke, C. R. *Mass Transfer*; McGraw-Hill: New York, 1975; pp 346-361.

(19) Schwartz, S. E.; White, W. H. *Adv. Environ. Sci. Technol.* **1983**, *12*, 1-116.

(20) Schwartz, S. E.; White, W. H. *Adv. Environ. Sci. Eng.* **1981**, *4*, 1-45.

(21) Liss, P. S. *J. Great Lakes Res.* **1976**, *2* (suppl. 1), 88, 126.

(22) Orel, A. E.; Seinfeld, J. H. *Environ. Sci. Technol.* **1977**, *11*, 1000.

(23) Durham, J. C.; Overton, J. H.; Aneja, V. P. *Atmos. Environ.* **1981**, *15*, 1059.

(24) Lee, Y.-N.; Schwartz, S. E. *J. Geophys. Res.* **1981**, *86*, 11971.

(25) Liljestrand, H. M.; Morgan, J. F. *Environ. Sci. Technol.* **1981**, *15*, 333.

[†] Present address: Department of Science Education, Ewa Women's University, Seoul, Korea.

The studies that have been made involving nitrous acid include indirect kinetic studies of nitrous acid decomposition and formation in the "mixed phase",^{26,27} where mass transfer across the phase boundary is involved, direct aqueous-phase kinetic studies using pulse radiolysis and flash photolysis,^{28,29} and absorption rate measurements in gas-liquid contactors.³⁰⁻³⁶ However, despite the numerous attempts, significant disagreements still exist among the rate constants, e.g., by as much as an order of magnitude.¹⁹

Concerning the measurement of the Henry's law solubility, the direct determination for gases that undergo reactive dissolution is inherently difficult because the gas-liquid systems are generally not maintained at equilibrium during measurement, and the data interpretation is frequently complicated by the mass-transport properties of the experimental configuration. For this reason, NO represents the only species among the oxides and oxyacids of nitrogen^{37,38} whose Henry's law constant has been accurately determined. For nitrous acid, there has been only one prior direct experimental determination, whereby Abel and Neusser³⁹ determined the Henry's law coefficient by measuring the equilibrium gas- and aqueous-phase concentrations of HNO₂, in the presence of excess NO to suppress the decomposition of nitrous acid. The value they obtained at 25 °C, extrapolated to zero ionic strength, was 28 M atm⁻¹. This value was corrected by Wayne and Yost⁴⁰ to 33 M atm⁻¹ to take into account the gas-phase dissociation of HNO₂ to NO and NO₂, which Abel and Neusser had acknowledged to be a potential source of experimental error.

Since the Henry's law coefficient is an equilibrium constant, an alternative method frequently employed to estimate this quantity is evaluating the free energy change of solution by using the relation

$$\Delta G^\circ_{\text{sol}} = \Delta_f G^\circ(X_{\text{aq}}) - \Delta_f G^\circ(X_{\text{g}}) = -RT \ln H_X \quad (3)$$

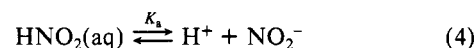
where $\Delta_f G^\circ$ is the standard free energy of formation, X represents the chemical species, H is the Henry's law constant, R is the universal gas constant, T is the absolute temperature, and subscripts aq and g denote aqueous phase and gas phase, respectively. Clearly, the degree of success of this approach depends on the availability and accuracy of the corresponding thermodynamic values. Recently Carta⁴¹ evaluated the Henry's law solubility of HNO₂ to be 59.2 M atm⁻¹ at 25 °C using a thermochemical cycle in conjunction with the experimental data of Theobald⁴² derived from his study of the heterogeneous equilibrium of gaseous nitric oxide and nitrogen dioxide with solutions of nitric and nitrous acids mixtures. Additionally, Schwartz and White²⁰ suggested a value of 49 M atm⁻¹ at 25 °C estimated by using eq 3 with values of $\Delta_f G^\circ(\text{HNO}_2(\text{g})) = -11.0 \text{ kcal mol}^{-1}$ and $\Delta_f G^\circ(\text{HNO}_2(\text{aq})) = -13.3 \text{ kcal mol}^{-1}$, recommended by the National Bureau of Standards (NBS) at that time.⁴³ Since then the value recom-

mended for $\Delta_f G^\circ(\text{HNO}_2(\text{aq}))$ was changed to $-12.1 \text{ kcal mol}^{-1}$,⁴⁴ and the calculated value of H_{HNO_2} should accordingly be changed to 6.4 M atm⁻¹.⁴⁵ The fact that this value is almost an order of magnitude lower than those estimated by Carta and determined experimentally by Abel and Neusser indicates that substantial uncertainty still exists in the value of the Henry's law solubility of HNO₂. Such uncertainty would also raise serious questions on the solubilities of NO₂, N₂O₃, and N₂O₄ evaluated by thermochemical cycles²⁰ that hinge on the solubility of HNO₂.

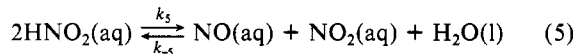
We report in this paper the determination of the Henry's law solubility and the aqueous decomposition kinetics of nitrous acid, i.e., the rate constants of reactions 1 and 2, by using a gas-liquid contactor apparatus of known phase-mixing properties and by following the change of the concentrations of pertinent nitrogen species present in the gas phase of this system as a function of time. The feasibility of this approach is, to a large measure, due to the fact that the rate of nitrous acid decomposition, which is second order in its own concentration, was suppressed by the use of extremely low concentrations of nitrous acid. The reduced rate of decomposition resulting from low nitrous acid concentration, i.e., $4.5 \times 10^{-5} \text{ M}$ for the kinetics study and $2.0 \times 10^{-6} \text{ M}$ for the solubility measurement, allowed the time dependence of the concentrations of the species involved to be easily measured and the mass-transport processes to be adequately delineated. Additional advantages associated with the low reagent concentrations are the facts that the simple oxides of nitrogen (NO and NO₂) are the dominant species and the concentrations of compound oxides, i.e., N₂O₃ and N₂O₄, are vanishingly small, thereby allowing the overall kinetic scheme to be simplified. Continuous detection of the nitrogen species of the system, which contained less than a total of $1 \times 10^{-6} \text{ mol}$ of material, was achieved by monitoring the concentrations of these species in the gas phase in contact with the liquid by use of a chemiluminescence NO_x detector.

Model

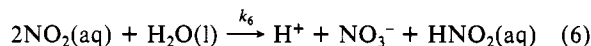
The reaction of nitrous acid in aqueous solution involves the acid-base dissociation



where K_a is the acid dissociation constant of nitrous acid, and the reversible decomposition to nitric oxide (NO) and nitrogen dioxide (NO₂)



where k_5 and k_{-5} are the forward and reverse rate constants, respectively. The NO₂ produced further undergoes hydrolysis to yield nitric and nitrous acid according to



where k_6 is the forward rate constant.

Henry's Law Solubility. The volatile species generated in the solution such as NO and NO₂ will redistribute into the gas volume that is in contact with the solution and establish a partition between the two phases according to Henry's law. When the contact of the two phases is achieved by convective mixing as is the case of an agitated gas-liquid reactor used in this work, the mass transport of a dissolved gas X in its redistribution can be envisioned to involve two steps:⁴⁶ from the bulk solution to the liquid surface and from

(26) (a) Abel, E.; Schmid, H. *Z. Phys. Chem.* **1928**, *132*, 55; *134*, 279; *136*, 430. (b) Abel, E.; Schmid, H.; Babad, S. *Z. Phys. Chem.* **1928**, *136*, 419, 430. (c) Abel, E.; Schmid, H.; Römer, E. *Z. Phys. Chem.* **1930**, *148*, 337.

(27) Komiyama, H.; Inoue, H. *J. Chem. Eng. Jpn.* **1978**, *11*, 25.

(28) (a) Grätzel, M.; Henglein, A.; Lilie, J.; Beck, G. *Ber. Bunsen-Ges. Phys. Chem.* **1969**, *73*, 646. (b) Grätzel, M.; Taniguchi, S.; Henglein, A. *Ber. Bunsen-Ges. Phys. Chem.* **1970**, *74*, 488.

(29) Treinin, A.; Hayon, E. *J. Am. Chem. Soc.* **1970**, *92*, 5821.

(30) Wendel, M. M.; Pigford, R. L. *AIChE J.* **1958**, *4*, 249.

(31) Kramers, H.; Blind, M. P. P.; Snoeck, E. *Chem. Eng. Sci.* **1961**, *14*, 115.

(32) Andrew, S. P. S.; Hanson, D. *Chem. Eng. Sci.* **1961**, *14*, 105.

(33) Hofmeister, H.-K.; Kohlhaas, R. *Ber. Bunsenges.* **1965**, *69*, 232.

(34) Kameoka, Y.; Pigford, R. L. *Ind. Eng. Chem. Fundam.* **1977**, *16*, 163.

(35) Komiyama, H.; Inoue, H. *Chem. Eng. Sci.* **1980**, *35*, 154.

(36) Lee, Y.-N.; Schwartz, S. E. *J. Phys. Chem.* **1981**, *85*, 840.

(37) Loomis, A. G. In *International Critical Tables*; McGraw-Hill: New York, 1928; Vol. 3, pp 255-261.

(38) Armor, J. N. *J. Chem. Eng. Data* **1974**, *19*, 82.

(39) Abel, E.; Neusser, E. *Monatsh. Chem.* **1929**, *53*, 855.

(40) Wayne, L. G.; Yost, D. M. *J. Chem. Phys.* **1951**, *19*, 41.

(41) Carta, G. *Ind. Eng. Chem. Fundam.* **1984**, *23*, 260.

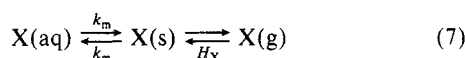
(42) Theobald, H. *Chem. Eng. Technol.* **1968**, *40*, 763.

(43) Wagman, D. D.; Evans, W. H.; Parker, V. B.; Halow, I.; Bailey, S. M.; Schumm, R. H. *NBS Tech. Note (U.S.)* **1968**, No. 270-3.

(44) Wagman, D. D.; Evans, W. H.; Parker, V. B.; Schumm, R. H.; Nuttall, R. L. *NBS Tech. Note (U.S.)* **1981**, No. 270-8.

(45) The decision to adjust a number of thermodynamic parameters concerning the HNO₂ system actually resulted from the fact that a fairly reliable determination of the absolute entropy of KNO₂(cr) had yielded $S^\circ(\text{NO}_2^-, \text{aq}) = 29.4 \pm 0.5 \text{ cal mol}^{-1} \text{ K}^{-1}$ (Mraw, S. C.; Boak, R. J.; Staveley, L. A. *Chem. Thermodynam.* **1978**, *10*, 359). Since it appeared unwarranted to adjust $\Delta_f H^\circ(\text{NO}_2^-, \text{aq})$, the new value of $S^\circ(\text{NO}_2^-, \text{aq})$ was reflected solely on $\Delta_f G^\circ(\text{NO}_2^-, \text{aq})$. Further, since the relation between HNO₂(g) and HNO₂(aq) was not considered to be well defined, no adjustment was propagated into the properties of the gaseous species (private communication from V. B. Parker to S. E. Schwartz, 1985).

the liquid surface to the gas phase, i.e.



where s denotes surface, and k_m , the stochastic rate coefficient for the convective mixing, is equivalent to chemical engineer's term, $k_L a$, as defined by the experimentally observed rate of physical absorption of gases into liquid, i.e.

$$\bar{R}a = k_L a [X(\text{s}) - X(\text{aq})] \quad (8)$$

where \bar{R} is the average rate of transfer per unit area, k_L is the physical mass-transfer coefficient, and a is the interfacial area per unit volume of liquid. In the two-film model describing gas transfer between the gas and liquid phases, the overall resistance K_L is given as the combination of gas- and liquid-phase resistance, i.e.

$$\frac{1}{K_L} = \frac{1}{k_L} + \frac{HRT}{k_G} \quad (9)$$

where k_G is the gas-phase mass-transfer coefficient.⁴⁶

For the purging-out of a dissolved species from a gas-liquid reactor under the assumptions of negligible gas-side resistance and the establishment of gas-liquid equilibrium at the interface with a uniform concentration in bulk liquid, the removal rate of dissolved gas X is given from mass conservation as

$$-d[X(\text{aq})]/dt = k_m[X(\text{aq})] - k_m H_X p_X = F_g p_X / (RTV_1) \quad (10)$$

where p_X is the partial pressure of X, F_g is the gas-flow rate, and V_1 is the liquid volume. The relation between the concentration of solute X in bulk solution and in gas phase at steady condition is derived from eq 10 as

$$[X(\text{aq})] = [H_X + F_g / (RTV_1 k_m)] p_X \quad (11)$$

In the absence of chemical reactions the rate of purging can be expressed as

$$-d[X(\text{aq})]/dt = (RTH_X V_1 / F_g + 1/k_m)^{-1} [X(\text{aq})] \quad (12)$$

or

$$-dp_X/dt = (RTH_X V_1 / F_g + 1/k_m)^{-1} p_X \quad (13)$$

The characteristic time of purging of a dissolved species is therefore obtained as

$$\tau = RTH_X V_1 / F_g + 1/k_m \quad (14)$$

This purging time constant, which can be determined either from the first-order decay of p_X in the once-through flow effluent gas or from the rate of $[X(\text{aq})]$ decrease, is seen to be comprised of two terms as controlled by the Henry's law constant of the species involved and the phase-mixing time constant characteristic of the physical configuration of the mixing apparatus and the experimental conditions employed.

One condition that must be satisfied in the determination of Henry's law constant using this purging technique is that the magnitudes of the two terms on the right-hand side of eq 14 are comparable or, preferably, that the first term is predominant, i.e.

$$\tau = RTH_X V_1 / F_g \quad \text{when } RTH_X V_1 / F_g \gg 1/k_m \quad (15)$$

It will be shown below that the convective mixing time constant τ_m ($\equiv 1/k_m$) characteristic of the gas-liquid reactor and the experimental conditions employed in the present work fall in such a range that eq 15 is valid provided that $H_X \gg 0.2 \text{ M atm}^{-1}$. For HNO_2 , whose Henry's law coefficient is estimated to be on the order of 50 M atm^{-1} ,²⁰ eq 15 is applicable and H_{HNO_2} can thus be determined directly from τ measured when purging out the HNO_2 . However, since nitrous acid is in rapid equilibrium with nitrite ion by reaction 4 and the solubility constant thus determined actually represents the effective Henry's law coefficient H^* , i.e.

$$H^* = H_{\text{HNO}_2} (1 + K_a / [H^+]) \quad (16)$$

the determination of the physical solubility of HNO_2 , i.e., H_{HNO_2} , requires a study of the pH dependence of H^* and the extrapolation of this value to $1/[H^+] = 0$.

It should be emphasized that for application of this technique a sufficiently low HNO_2 concentration must be used to minimize the effect of HNO_2 decomposition. In other words, the rate of the second-order decomposition of HNO_2 must be kept small compared to that of purging such that the predominant mechanism for the loss of the aqueous HNO_2 is governed by the physical mass transfer into the gas phase of this species and not by chemical reactions. At an initial concentration of $2 \times 10^{-6} \text{ M}$, HNO_2 is expected to decompose at a negligibly small rate compared to the purging rate, thereby satisfying the required condition. This expectation will be shown to be consistent with the values of rate constant k_5 and the purging rate constant $1/\tau$ determined in this work.

Rate Constant Measurement. At higher initial concentrations of nitrous acid (e.g., $5 \times 10^{-5} \text{ M}$), appreciable decomposition is expected to take place. Since the decomposition products, NO and NO_2 , will also be purged out along with HNO_2 , the concentrations of these species being governed by chemical reactions as well as physical purging, kinetic information on reactions 5 and 6 can be extracted from the knowledge of the partial pressures of these species in the effluent gas as described below.

By applying the steady-state approximation to $\text{NO}(\text{aq})$ and $\text{NO}_2(\text{aq})$, we obtain from eq 5-7 and 12

$$d[\text{NO}(\text{aq})]/dt = 0 = k_5 [\text{HNO}_2(\text{aq})]^2 - k_{-5} [\text{NO}(\text{aq})] \times [\text{NO}_2(\text{aq})] - (RTH_{\text{NO}} V_1 / F_g + 1/k_m)^{-1} [\text{NO}(\text{aq})] \quad (17)$$

$$d[\text{NO}_2(\text{aq})]/dt = 0 = k_5 [\text{HNO}_2(\text{aq})]^2 - k_{-5} [\text{NO}(\text{aq})] \times [\text{NO}_2(\text{aq})] - 2k_6 [\text{NO}_2(\text{aq})]^2 - (RTH_{\text{NO}_2} V_1 / F_g + 1/k_m)^{-1} [\text{NO}_2(\text{aq})] \quad (18)$$

where the last terms in these equations represent the purging rate of NO and NO_2 , respectively. From eq 17 and 18, and substituting p_X for $[X(\text{aq})]$ using eq 11, we further obtain

$$k_6 = Ck_m(p_{\text{NO}} - p_{\text{NO}_2}) / [2(H_{\text{NO}_2} + C)^2 p_{\text{NO}_2}^2] \quad (19)$$

where $C = F_g / RTV_1 k_m$, a constant governed only by the experimental conditions employed. An expression for k_5 can be derived with the assumption that $H_{\text{HNO}_2} \gg F_g / RTV_1 k_m$ (a condition that will be demonstrated below to be consistent with the experimental results) by substituting eq 11 into eq 17 as

$$k_5 = Ck_m p_{\text{NO}} / [(H_{\text{HNO}_2} p_{\text{HNO}_2})^2 - (H_{\text{NO}} + C) \times (H_{\text{NO}_2} + C) p_{\text{NO}} p_{\text{NO}_2} / K_5] \quad (20)$$

where $K_5 = k_5/k_{-5}$. Consequently, the value of k_6 can be determined from the partial pressures of NO and NO_2 in the effluent gas, along with the known values of C and H_{NO_2} . Also, the values of k_5 and k_{-5} can be obtained in a similar fashion from the partial pressures of NO, NO_2 , and HNO_2 , with K_5 as an adjustable parameter.

Experimental Section

Two sets of experiments have been conducted in this study: one for the determination of the solubility of nitrous acid alone and the other for the determination of the reaction kinetics of nitrous acid decomposition as well as the solubilities of the species involved. In addition, the convective mixing rate coefficient k_m of the gas-liquid reactor used in this study was determined by using CO_2 uptake. The apparatus and procedures used for the latter experiment are similar to those reported earlier.³⁶

Materials. Reagent grade inorganic salts NaNO_2 , Na_2SO_4 (both from Fisher), and KCl (Baker) were used without further purification. Sulfuric acid and sodium hydroxide were standard volumetric solutions obtained as Acculute from Anachemia (Champlain, NY) and diluted to desired concentrations before use. Nitrogen gas (ultrahigh purity (UHP), 99.999%, Liquid Carbonic) and bone-dry CO_2 (99.8%, Matheson) were also used

(46) Danckwerts, P. V. *Gas-Liquid Reactions*; McGraw-Hill: New York, 1970.

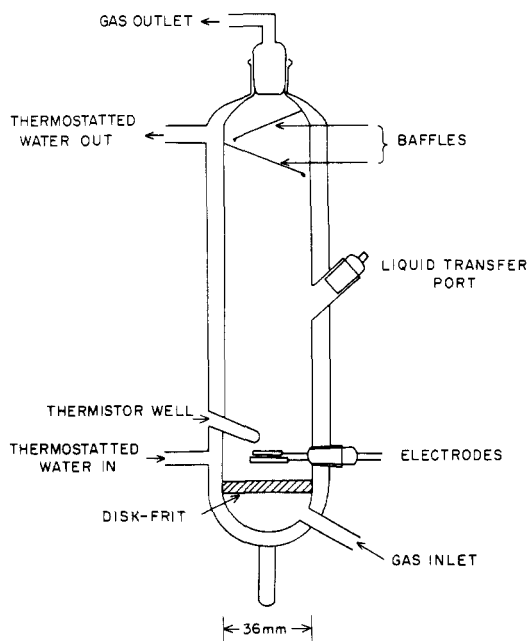


Figure 1. Gas-liquid reactor.

without purification. A bottle of standard NO for calibration purpose was obtained from NBS (47.6 ppm, SRM No. 1683B). Millipore Milli-Q filtered water (resistivity $> 16 \text{ M}\Omega \text{ cm}$ at 25°C) was used for all of the experiments.

Gas-Liquid Reactor. The bubbler-type gas-liquid reactor equipped with a water jacket for temperature control consists of a 3.6-cm i.d. Pyrex cylindrical tube and a fritted-disk bottom (Figure 1). The UHP N_2 once-through flow passes through the liquid as finely divided bubbles by entering the cell through the fritted-disk bottom of the reactor. Efficient mixing of the gas and liquid was accomplished by the large interfacial area created by the large number of bubbles and the mechanical agitation resulting from the upward motion of the bubbles. Two glass baffles attached at the top of the reactor prevent any large water droplets from escaping the reactor. The temperature of the reactor during experiments was maintained constant within $\pm 0.05^\circ\text{C}$ by circulating thermostated water through the water jacket by using a refrigerated circulating bath (Endocal RTE-9, Neslab). Ports allowing for liquid transfer, the conductivity electrodes, and a temperature probe are also shown in Figure 1.

Determination of the Concentrations of Gaseous Nitrogen Species. The gas-phase concentrations of NO, NO_2 , and HNO_2 purged out from the reactor by the carrier gas N_2 were determined by a high-sensitivity O_3 -chemiluminescence NO_x detector (Model 14B/E, TECO). The principle of operation of this NO_x detector is the detection of the light emitted from electronically excited NO_2 molecules produced from the $\text{NO}-\text{O}_3$ reaction. Consequently, under normal circumstances, NO is the only species that is being detected, and this mode of operation is referred to as NO channel. So that NO_2 and HNO_2 can also be detected, these species must first be reduced to NO, for which purpose a molybdenum catalytic converter is employed. With the converter employed, the signal obtained represents the total concentration of NO, NO_2 , and HNO_2 , and this mode of operation is referred to as NO_y ($\equiv \text{NO} + \text{NO}_2 + \text{HNO}_2$) channel. The difference between the NO_y and NO channels represents $\text{NO}_2 + \text{HNO}_2$.

The sensitivity of this commercial instrument has been improved to exhibit a limit of detection of $\sim 3 \times 10^{-10} \text{ atm}$ by a number of modifications, principal among which are utilization of a high-speed vacuum pump (Type 1012A, CIT-Alcatel) to increase the sample flow rate to ca. 1 L/min (at 1 atm) and the incorporation of an enlarged reaction chamber to optimize the O_3 -NO reagent mixture residence time.⁴⁷ The pressure of the reaction

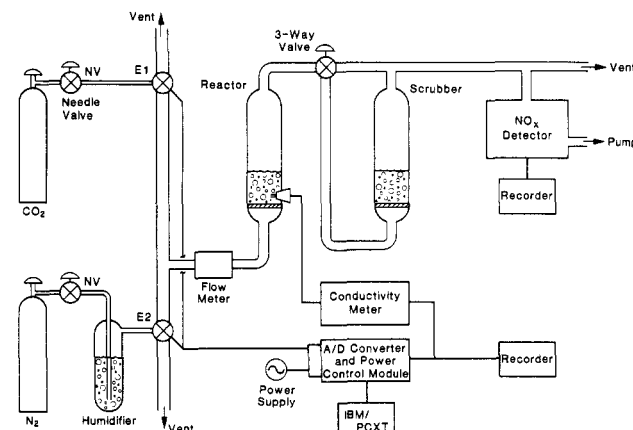


Figure 2. Schematic diagram of experimental setup and apparatus.

chamber was maintained typically at 0.07 atm. The calibration of the NO_x detector was achieved by using an NBS standard NO dynamically diluted with nitrogen gas to the desired concentration range, i.e., 5×10^{-9} to $1 \times 10^{-6} \text{ atm}$. The sensitivity of the NO_y channel, which reflects primarily the efficiency of the catalytic converter, was also examined by using the same NBS standard NO gas following oxidation to NO_2 using excess amount of ozone generated from a gas calibrator (Model 8550, Monitor Labs). The sensitivities of the NO and NO_y channels were found to be identical.

Experimental Setup. The experimental setup, which consists of compressed UHP N_2 , humidifier, the gas-liquid reactor, gas scrubbers, the NO_x detector, and the necessary plumbing, is shown schematically in Figure 2. The nitrogen carrier gas was humidified before entering the reactor to minimize the loss of liquid from evaporation. The humidifier and the reactor were maintained at the same temperature, and no noticeable change of liquid volume in the reactor was found for up to several hours by observing the conductivity of a dilute KCl solution in the reactor. The gas flow rate was measured using a flow meter (No. 448-309, Fisher and Porter), which was calibrated by a water displacement method.

The pH of the reaction mixtures was measured typically at the conclusion of a run for samples taken out from the gas-liquid reactor by using a research grade pH meter (Model 4500, Beckman) in conjunction with a semimicro combination electrode (Model 810300, Orion Research). The electrical conductivity of solutions was measured continuously during runs by using a conductivity meter (Electromark 4402, Markson) equipped with a pair of Pt electrodes fused on a ground-glass joint and immersed in the reaction mixture (Figure 1).

For facilitation of the determination of the mass-transfer coefficient of the gas-liquid reactor by CO_2 adsorption, the gas entering the reactor can be switched instantaneously between two different sources (i.e., N_2 and CO_2) controlled by two electrically coupled three-way solenoid valves (Model 802-2324, MACE). Effort was also made to minimize the length of the Teflon tubing and the number of valves used in the gas plumbing system downstream of the reactor to minimize any possible loss of HNO_2 arising from surface interactions.

Experimental Procedure. To prepare for an experimental run, we first rinsed the reactor thoroughly with deionized water and rid it of any visible water droplets by aspiration. This procedure allows the entire reactor, including the entrance region below the fritted disk to be cleaned. Following that, the N_2 flow was turned on, and the reactor was further rinsed by three to four portions of $\sim 20 \text{ mL}$ of water until the conductivity reading reached the background value. The waste solution was removed from the reactor by aspiration; it was found that 0.4 mL of water invariably remained in the reactor after cleaning, presumably the amount of water trapped between the two platinum electrodes. With the N_2 carrier gas continually flowing, the desired amount of water was added into the reactor followed by the addition of a predetermined amount (ca. $100 \mu\text{L}$) of sodium nitrite stock solution

(47) Kelly, T. J. *Brookhaven National Laboratory Informal Report*, BNL-38000, 1986.

((2–50) × 10⁻⁴ M) into the reactor to yield a final NaNO₂ solution of the desired concentration. After the temperature of the reaction mixture reached equilibrium, a small volume of sulfuric acid (typically 1% of the total volume) was added to acidify the solution and to initiate the reaction. The nitrous acid and nitrogen oxides resulting from the acidification and decomposition were purged from the solution by the nitrogen carrier gas, and the effluent gas was continuously analyzed by the NO_x detector on the proper channel. The concentration of the nitrogen species as a function of time was recorded on a strip chart recorder.

For the solubility measurement experiments, an extremely low initial concentration of sodium nitrite (i.e., 2 × 10⁻⁶ M) was used to suppress the nitrous acid decomposition. Under this low reagent concentration condition the effluent gas was monitored only for NO_y, because the concentration of NO purged was too small to discern (typically <5% of NO_y). This set of experiments was performed for four liquid volumes between 5 and 40 mL at three different pH values between 2.13 and 3.33, all at 22 °C. Some of the runs at higher pH values were conducted with their solution ionic strengths adjusted to match that corresponding to pH 2.13 (μ = 0.014) by adding Na₂SO₄ or KCl. In addition, experimental runs were performed at three other temperatures (i.e., 0.2, 10.0, and 30.0 °C) at V_l = 10.5 mL and pH 2.13 for the determination of the temperature dependence. A N₂ gas-flow rate of 2.15 L min⁻¹ was used for all the experiments.

For the kinetics study, a higher initial concentration of nitrous acid was used (i.e., 4.5 × 10⁻⁵ M) to promote the nitrous acid decomposition and to allow the temporal behavior of NO concentration of the effluent gas to be examined. For these experimental runs, the effluent gas was determined for both NO and NO_y within the same run with the NO_x detector switched alternately between the NO and NO_y channel. To further distinguish NO₂ from HNO₂, we connected a gas scrubber similar in construction to the gas-liquid reactor (see Figure 2) downstream of the reactor to remove HNO₂, thereby allowing NO + NO₂ to be measured in the NO_y channel. It should be pointed out that the scrubber is either present or absent for the entire duration of a given experimental run. The information on the concentrations of NO₂ and HNO₂ was therefore obtained from a pair of runs with and without the scrubber in place but under otherwise identical experimental conditions. The removal efficiency for HNO₂ by the scrubber containing 1 × 10⁻³ M NaOH solution was found to be greater than 99% as determined by observing the signal change of the NO_y channel with a second scrubber connected in series with the primary scrubber. The kinetics experiments were performed for three different liquid volumes (i.e., 15, 25, and 40 mL) at three temperatures (i.e., 10.0, 22.0, and 30.0 °C) at pH 2.13.

Determination of Convective Mixing Rate. The stochastic convective mixing rate coefficient k_m of the gas-liquid reactor, which affects the mass transport of a solute species, plays an important role in the experiments conducted in this work. As can be seen from the Model section, knowledge of the value of this parameter would allow the intrinsic chemical properties, such as solubility and rate coefficients, to be determined from the overall measurements. We determined the value of k_m for the reactor employed here by measuring the rate of CO₂ uptake because this absorption process is essentially governed by convective mixing alone due to the rather low solubility of CO₂ (cf. eq 14). Furthermore, the aqueous-phase CO₂ concentration change during the uptake can be readily detected by measuring the electrical conductivity change of the solution resulting from the CO₂ hydrolysis products, H⁺ and HCO₃⁻. This method has been described in detail previously,³⁶ and only a brief discussion is given below.

The CO₂ absorption experiment was initiated by switching instantaneously the source gas into the reactor from N₂ to CO₂. The time dependence of the buildup of the dissolved CO₂ as the pure CO₂ bubbling through the liquid is given by⁴⁶

$$[\text{CO}_2(\text{aq})]_t = [\text{CO}_2(\text{aq})]_\infty (1 - e^{-t/\tau}) \quad (21)$$

where τ is characteristic time of the uptake as described by eq 14. Since a small portion of the dissolved CO₂ is rapidly hy-

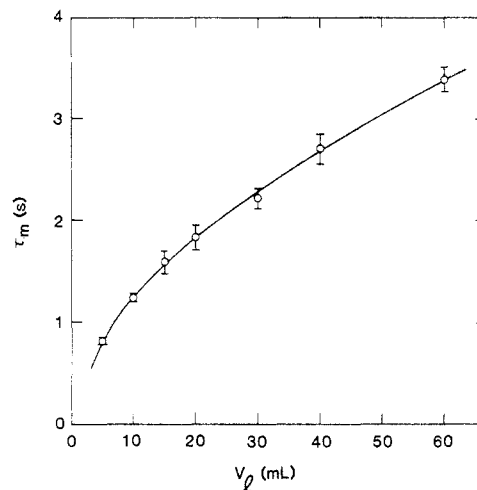


Figure 3. Liquid volume dependence of the characteristic time of mixing of the bubbler reactor at 22 °C and gas-flow rate of 35 cm³ s⁻¹. Each point represents the average of four or more measurements, and the error bar is the standard deviation.

drollyzed⁴⁸ to produce the ionic species H⁺ and HCO₃⁻, whose concentrations are in proportion to that of the dissolved CO₂, eq 21 can be rewritten in terms of conductivity, viz.

$$\kappa_t^2 = \kappa_\infty^2 (1 - e^{-t/\tau}) \quad (22)$$

From a plot of $\ln(\kappa_\infty^2 - \kappa_t^2)$ as a function of t , the value of $-\tau$ is obtained as the inverse of the slope of the resulting straight line. Consequently, k_m can be calculated from eq 14 with the known solubility of CO₂. It may be noted that since the process of the CO₂ uptake is rather rapid under the current arrangement, which normally spans only a few seconds, a computer-assisted data acquisition and handling technique was used to control the uptake experiments by switching the source gas from N₂ to CO₂ and to record the subsequent conductivity change immediately thereafter. This set of experiments was performed at seven different liquid volumes varying between 5 and 60 mL and at 22.0 °C with the gas-flow rate maintained at 2.15 L min⁻¹.

Results and Discussion

Convective Mixing Time. The characteristic time (τ) for CO₂ uptake of the gas-liquid reactor was determined by using eq 22 from the observed conductivity change accompanying the CO₂ absorption. The convective mixing time (τ_m) characteristic of the reactor was calculated from eq 14 by using $H_{\text{CO}_2} = 3.4 \times 10^{-2}$ M atm⁻¹ (22 °C).³⁷ The τ_m values thus obtained are plotted in Figure 3 as a function of the liquid volume, and it is noted that they range between 1 and 3 s. Each point represents the average of four or more measurements, and the error bars indicate standard deviations and resulted in an estimated accuracy of ±10%. In view of the rather small values of τ_m , it is recognized that the rate of purging of HNO₂ is primarily governed by the first term of eq 14, consistent with the assumption that eq 14 would be suitable for determining H_{HNO_2} provided that the solubility of HNO₂ is 3 M atm⁻¹ or greater. However, the second term would become more important for the purging of much less soluble gases, such as NO and NO₂.

Henry's Law Solubility of Nitrous Acid. The Henry's law solubility of nitrous acid was calculated from the purging rate of N(III) determined from the decay of p_{HNO_2} in the effluent gas as monitored by the NO_x detector. In these experiments where the total initial N(III) concentration was maintained at 2 × 10⁻⁶ M, NO concentration purged from the solution was found to constitute less than 5% of the NO_y signal and was too small to be determined accurately. Consequently, only the NO_y concentration was monitored, and the signal was attributed entirely to HNO₂. A typical trace of the concentration of HNO₂ in the

(48) Eigen, M.; Kruse, W.; Maass, G.; DeMaeyer, L. In *Progress in Reaction Kinetics*; Porter, G., Ed.; Pergamon: Oxford, 1964, pp 286–318.

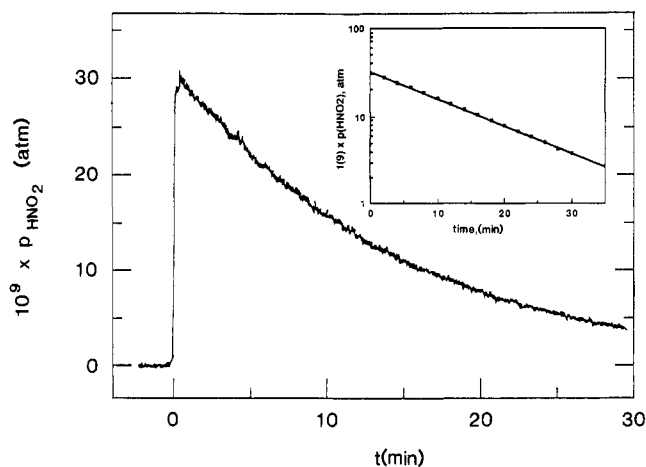


Figure 4. Temporal profile of HNO₂ concentration during the purging process for solubility measurement. Experimental conditions: $F_g = 35 \text{ cm}^3 \text{ s}^{-1}$, $V_l = 20.6 \text{ mL}$, pH 2.13, temperature = 22.0 °C, $[\text{NaNO}_2]_0 = 2.0 \times 10^{-6} \text{ M}$. The first-order plot of the data is shown in the inset.

TABLE I: Liquid Volume Dependence of the Characteristic Time of Purging of Nitrous Acid and Effective Henry's Law Coefficients ($T = 22 \text{ }^\circ\text{C}$)^a

V_l, cm^3	$\tau_{\text{N(III)}}, \text{s}$		
	pH 2.13	pH 3.03	pH 3.33
5.45	240 ± 5 (0.2%)	361 ± 17	471 ± 14
10.5	463 ± 10 (0.8%)	666 ± 19 (0.7%)	899 ± 21 (0.6%)
20.6	894 ± 13 (2.4%)	1327 ± 23 (2.2%)	1759 ± 37 (1.6%)
40.8	1786 ± 41 (5.1%)	2621 ± 66 (4.6%)	3421 ± 111 (3.3%)
$H^*, \text{M atm}^{-1}$	64 ± 3	95 ± 5	124 ± 6

^a Each $\tau_{\text{N(III)}}$ value given represents the average and the standard deviation of four or more measurements. Values in parentheses represent the magnitude of corrections made for HNO₂ decomposition.

effluent gas purged from the reactor as a function of time is shown in Figure 4. The first-order plot of the data, i.e., $\ln p_{\text{HNO}_2}$ versus time, exhibited linearity for three half-lives (inset of Figure 4); the characteristic time of purging of N(III), $\tau_{\text{N(III)}}$, was taken as the inverse of the slope of these straight lines.

Before carrying out the data reduction and interpretation, we should point out that although the initial N(III) concentration was kept as low as would be allowed by the sensitivity of the NO_x detector, minor corrections for aqueous-phase nitrous acid decomposition may still be necessary under certain conditions. The effects of this decomposition include a faster decay rate of aqueous HNO₂ than can be accounted for by physical purging alone and an increased level of NO_y signal as it also includes the less soluble decomposition products NO and NO₂. To evaluate the effect of HNO₂ decomposition on these solubility measurements, we performed a self-consistent examination in which the reaction system was numerically simulated using the solubility and the reaction rate constants determined in this study (see below for details of simulation). By comparing $\tau_{\text{N(III)}}$ calculated from the simulated NO_y concentration and $\tau_{\text{N(III)}}$ determined experimentally, we obtained the correction factor. Although this correction turned out to be quite minor, being less than 5% under the worst conditions (see Table I), the observed p_{NO_y} was nonetheless corrected prior to analysis. The deduction of the Henry's law constant of HNO₂ from the results of the purging out experiments with low initial HNO₂ concentration is given below.

Liquid Volume Dependence of τ . The values of $\tau_{\text{N(III)}}$ determined at three different pH values and at four different liquid volumes for each pH at 22 °C are given in Table I, each point being the average of four or more individual measurements. The plots at each pH of $\tau_{\text{N(III)}}$ as a function of liquid volume shown in Figure 5 exhibit a linear relationship between these two quantities, and the least-squares best fits are seen to pass through the origin within experimental uncertainties. These observations are in conformity with eq 15 and suggest that the purging technique and the conditions employed are applicable for the purpose

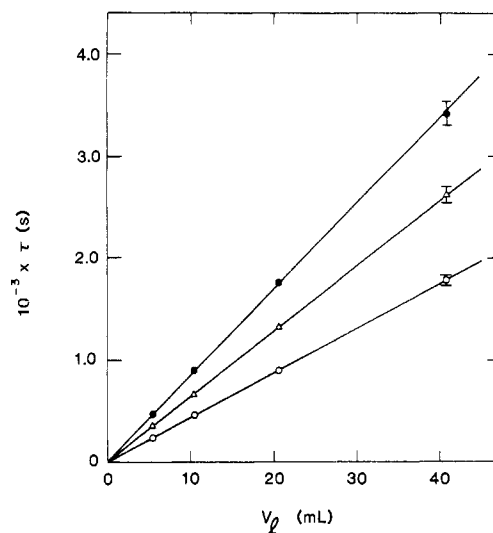


Figure 5. Liquid volume dependence of the characteristic time of purging of nitrous acid for three different pH values at 22.0 °C and gas-flow rate of 35 cm³ s⁻¹. Each point is the average of four or more measurements, and the error bar is the standard deviation of average. The error bar is not shown when it is equal to or smaller than the symbol size: (○) pH 2.13; (Δ) pH 3.03; (●) pH 3.33.

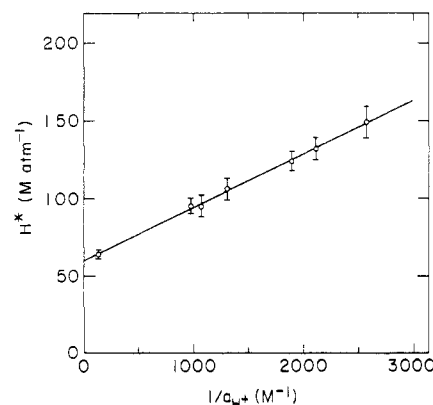


Figure 6. pH dependence of the effective Henry's law coefficient of nitrous acid at 22.0 °C and ionic strength 0.014. The error bars indicate the standard deviations of the means.

TABLE II: pH Dependence of the Effective Henry's Law Coefficients of Nitrous Acid Determined at $\mu = 0.014$ and 22.0 °C

$1/a_{\text{H}^+}, \text{M}^{-1}$	$H^*, \text{M atm}^{-1}$	$1/a_{\text{H}^+}, \text{M}^{-1}$	$H^*, \text{M atm}^{-1}$
133 ± 3	64 ± 3	1897 ± 18	124 ± 6 ^a
974 ± 23	95 ± 5 ^a	2113 ± 20	132 ± 7 ^b
1072 ± 25	95 ± 7 ^b	2576 ± 24	149 ± 10 ^c
1303 ± 30	106 ± 7 ^c		
$H_{\text{HNO}_2}, \text{M atm}^{-1}$		60 ± 3	
K_a, M		$(5.8 \pm 0.4) \times 10^{-4}$	
K_a^o, M		$(5.0 \pm 0.4) \times 10^{-4}$	

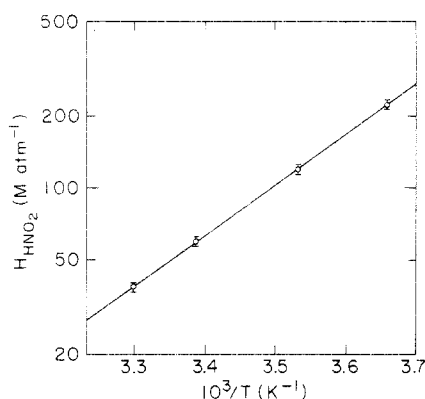
^a Results from Table I after correction for $1/a_{\text{H}^+}$ to have K_a value at $\mu = 0.014 \text{ M}$. ^b Ionic strength adjusted by KCl. ^c Ionic strength adjusted by Na₂SO₄.

of determining H_{HNO_2} . The effective Henry's law coefficient H^* for the several pH values calculated from the slope of the fitted line according to eq 15 are listed also in Table I.

pH Dependence of H^* . Since the effective Henry's law coefficient H^* is a function of hydrogen ion concentration as defined by eq 16, the study of its pH dependence would permit the values of H_{HNO_2} and the acid dissociation constant of HNO₂, K_a , to be determined. In Table II are listed the values of H^* determined in the pH range 2.13–3.33 with the ionic strength μ maintained constant at 0.014. It should be noted that some of the results obtained from the liquid volume dependence study (Table I) at lower ionic strengths are also included in Table II after corrections

TABLE III: Temperature Dependence of Henry's Law Coefficient of Nitrous Acid

temp, °C	H_{HNO_2} , M atm ⁻¹
0.2 ± 0.1	223 ± 11
10.0 ± 0.1	121 ± 6
22.0 ± 0.1	60 ± 3
30.0 ± 0.1	38 ± 2

**Figure 7.** Temperature dependence of Henry's law coefficient of nitrous acid. The error bars indicate the standard deviations of the means.

were made for ionic strength to correspond to $\mu = 0.014$ (see below). The pH dependence of H^* is displayed in Figure 6 by plotting H^* as a function of $1/a_{\text{H}^+}$ according to eq 16, where we adopted the convention that pH measures the activity of the hydrogen ion; the straight line represents the least-squares best fit to the data. From this straight line $H_{\text{HNO}_2} = 60 \pm 3 \text{ M atm}^{-1}$ is obtained as the intercept and $K_a = (5.8 \pm 0.4) \times 10^{-4} \text{ M}$ is determined from the slope. These values all correspond to $T = 22.0 \pm 0.1 \text{ }^\circ\text{C}$. The corresponding free energy of solution of nitrous acid in water, $\Delta G_{\text{sol}}^\circ$, at $22 \text{ }^\circ\text{C}$ is $-2.40 \pm 0.03 \text{ kcal mol}^{-1}$.

Since the thermodynamic acid dissociation constant at zero ionic strength K_a° is related to K_a by

$$K_a^\circ = a_{\text{H}^+}[\text{NO}_2^-]\gamma/[\text{HNO}_2] = \gamma K_a \quad (23)$$

where γ is the activity coefficient of NO_2^- , K_a° can be determined from K_a with a knowledge of γ . It may be noted that we have assumed a unit activity coefficient for nonionic species, i.e., HNO_2 . Since the activity coefficient of NO_2^- at low ionic strength can be estimated from the Debye-Hückel limiting law, i.e.

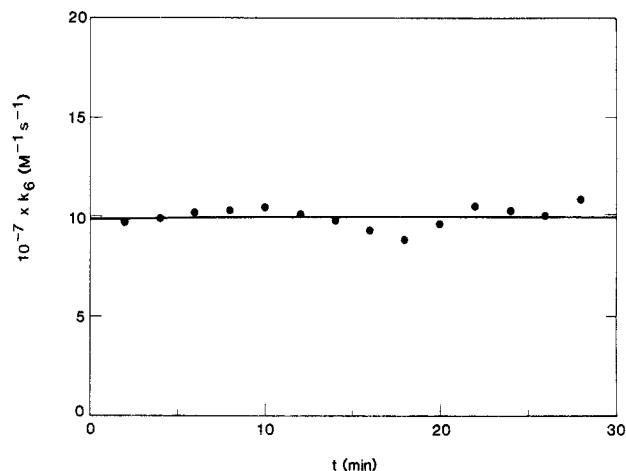
$$\log \gamma = -0.51z^2\mu^{1/2} \quad (24)$$

where z is charge of the ionic species, γ is evaluated to be 0.87 for $\mu = 0.014$ and $K_a^\circ = 5.0 \times 10^{-4} \text{ M}$ is obtained ($22 \text{ }^\circ\text{C}$). The value of K_a° corresponding to $25 \text{ }^\circ\text{C}$ is calculated to be $5.3 \times 10^{-4} \text{ M}$ by using $\Delta H^\circ = 3.5 \text{ kcal mol}^{-1}$ for the dissociation of HNO_2 ,⁴³ and this value agrees well with those reported in literature.⁴⁹⁻⁵¹

Temperature Dependence of H_{HNO_2} . The Henry's law coefficient of nitrous acid was determined at four different temperatures in the range $0.2\text{--}30 \text{ }^\circ\text{C}$. These values of H_{HNO_2} were derived from their corresponding H^* values determined at $V_1 = 10.5 \text{ mL}$ and pH 2.13 by using an initial $[\text{HNO}_2]$ of $2.0 \times 10^{-6} \text{ M}$. It is noted that an advantage of using a small liquid volume is the fact the correction for HNO_2 decomposition on the observed $\tau_{\text{N(III)}}$ is negligibly small (less than 1%; see Table I). To correct for the dissociation of nitrous acid, we used eq 16 with appropriate K_a values adjusted for each corresponding temperature calculated using $K_a(22^\circ\text{C}) = 5.8 \times 10^{-4} \text{ M}$ and $\Delta H^\circ = 3.5 \text{ kcal mol}^{-1}$.⁴³ The results are given in Table III. The Arrhenius type plot of the data, i.e., $\ln H_{\text{HNO}_2}$ versus $1/T$, shown in Figure 7, exhibits a linear relationship. The least-squares best fit of the data, represented by the straight line, yields $\Delta H_{\text{sol}}^\circ = -9.7 \pm 0.3 \text{ kcal mol}^{-1}$ and $\Delta S_{\text{sol}}^\circ = -24.8 \pm 0.7 \text{ cal mol}^{-1} \text{ K}^{-1}$.

TABLE IV: Rate Constants Determined at $22.0 \text{ }^\circ\text{C}$

V_1 , mL	k_5 , M ⁻¹ s ⁻¹	$10^{-8}k_{-5}$, M ⁻¹ s ⁻¹	$10^{-7}k_6$, M ⁻¹ s ⁻¹
15.6	14.4	1.62	6.7
25.7	13.4	1.68	9.7
40.8	12.4	1.43	8.8
av	13.4 ± 1.0	1.58 ± 0.13	8.4 ± 1.5

**Figure 8.** Calculated k_6 values as a function of time for a selected purging process. The straight line is drawn at the average value of k_6 . Experimental conditions: $F_g = 35 \text{ cm}^3 \text{ s}^{-1}$, $V_1 = 25.7 \text{ mL}$, pH 2.13, temperature = $22.0 \text{ }^\circ\text{C}$, $[\text{NaNO}_2]_0 = 4.4 \times 10^{-5} \text{ M}$.

Reaction Kinetics. As discussed in the Model section, knowledge of the concentrations of NO and NO_2 purged from the gas-liquid reactor resulting from HNO_2 decomposition would permit the kinetics of reaction 5 and 6 to be determined. To promote the decomposition of HNO_2 for the kinetic study, we employed an initial concentration of N(III) of $4.5 \times 10^{-5} \text{ M}$ to yield levels of NO and NO_2 that can be measured precisely. It also results in a decay kinetics with a characteristic time that is convenient to measure.

To determine the rate constant k_6 using eq 19, we measured the concentrations of NO and NO_2 in the effluent gas with the HNO_2 scrubber in place (Figure 2) and with the NO_x detector alternately detecting NO and NO_y . It should be noted that by including the scrubber in the flow system, the pressure of the reactor was found to increase slightly over the atmospheric pressure, i.e., by $\sim 8\%$. Consequently, eq 19 should be modified to

$$k_6 = Ck_m(p_{\text{NO}} - p_{\text{NO}_2})/[2(1.08H_{\text{NO}_2} + C)^2p_{\text{NO}_2}] \quad (25)$$

to take into account this pressure variation. The values of k_6 determined at three different liquid volumes are given in Table IV; the average is $8.4 \times 10^7 \text{ M}^{-1} \text{ s}^{-1}$ ($22.0 \text{ }^\circ\text{C}$), and the estimated uncertainty is $\pm 20\%$. The value of H_{NO_2} selected for determining k_6 is $2.0 \times 10^{-3} \text{ M atm}^{-1}$.^{37,38} Since the value of H_{NO_2} has not been unequivocally established, the value selected here represents the one recommended by Schwartz and White in their comprehensive review,²⁰ i.e., $1.0 \times 10^{-2} \text{ M atm}^{-1}$. However, it may be pointed out that the value of k_6 calculated is quite insensitive to the value of H_{NO_2} assigned. For example, with the value $7 \times 10^{-3} \text{ M atm}^{-1}$, which represents a $\sim 30\%$ change in H_{NO_2} , the value of k_6 was found to change by only 5%. A typical example showing the internal consistency of the calculated k_6 values corresponding to each set of data (i.e., in terms of p_{NO} and p_{NO_2}) in a single run is exhibited in Figure 8.

To determine the rate constants k_5 and k_{-5} for the reversible decomposition of HNO_2 , we conducted experiments to determine the partial pressures of NO, NO_2 , and HNO_2 of the effluent gas under the same conditions as those used to determine k_6 , except that the HNO_2 scrubber was not used. Under this arrangement, the partial pressures of NO and NO_y were experimentally determined by using the NO and NO_y channels, respectively. The partial pressure of NO_2 , on the other hand, was calculated from the observed p_{NO} by using eq 19 with the previously determined

(49) Schmid, H.; Marchgraber, R.; Dunkl, F. *Z. Elektrochem.* **1937**, *43*, 337.(50) Vassian, E. G.; Eberhardt, W. H. *J. Phys. Chem.* **1958**, *62*, 84.(51) Lee, Y.-N.; Lind, J. A. *J. Geophys. Res.* **1986**, *91*, 2793.

TABLE V: Temperature Dependence of Rate Constants

temp, °C	$k_5, \text{M}^{-1} \text{s}^{-1}$	$10^{-8}k_{-5}, \text{M}^{-1} \text{s}^{-1}$	$10^{-7}k_6, \text{M}^{-1} \text{s}^{-1}$
10.0	3.46	1.98	14.7
22.0	13.4	1.58	8.4
30.0	28.6	1.67	7.76

k_6 value. The value of p_{HNO_2} was then calculated from the measured NO_y, NO, and NO₂ concentrations. For each set of data within a kinetic run, k_5 was calculated from eq 20 with K_5 treated as an adjustable parameter. The final K_5 value was chosen as the one that provided the best agreement of k_5 values calculated among the entire set of data. The values of k_5 and k_{-5} evaluated this way are also shown in Table IV; the average values of k_5 and k_{-5} are $13.4 \text{ M}^{-1} \text{ s}^{-1}$ and $1.6 \times 10^8 \text{ M}^{-1} \text{ s}^{-1}$, respectively.

The kinetics study was also performed at two other temperatures, namely, 10 and 30 °C. The purpose of determining the values of k_5 , k_{-5} , and k_6 at these temperatures was to provide the necessary input for the evaluation of the correction factors resulting from HNO₂ decomposition in the solubility measurements. It should be noted that these values may have considerable uncertainties because k_m values for 22 °C were used in deriving the rate constants. Although such uncertainties preclude determining the activation energy, these values are considered to be sufficiently accurate for the evaluation of the correction factors because they turned out to be quite small in magnitude. The results are shown in Table V along with that obtained for 22 °C.

Numerical Simulation. To test the validity of the kinetic scheme put forward in this study, we numerically simulated the entire reaction system including both the chemical reactions and the physical mass transfer by solving rate equations simultaneously for each species involved using the solubility coefficients, rate constants, and mixing time constants determined in this study. The simulation program consists of a set of differential equations describing the concentration change of each species involved and does not entail the steady-state approximation. Most simulation runs were performed with time segments of 0.1 s for the evaluation of the stepwise concentration changes, and a shorter time segment did not lead to any perceptible improvement. The temporal profiles of partial pressures of NO and NO₂ in the effluent gas as calculated from the simulation are presented in Figure 9, together with the experimentally obtained results. The fact that the calculated results exhibit good agreement with experimental data establishes the validity of the kinetic model based upon steady-state concentrations of NO(aq) and NO₂(aq).

This numerical simulation was also carried out for the condition of low initial concentration of nitrous acid to determine the correction factor appropriate for the solubility measurements described earlier. The correction factors were calculated as the percentage difference between the calculated p_{HNO_2} and the overall observed p_{NO_y} , which was assumed to be solely responsible by HNO₂ in the solubility measurements because the levels of NO and NO₂ were too low to be measured precisely. Although the correction factors are relatively small, the maximum being ~5% (see Table I), the time dependence of p_{NO_y} of the effluent gas with which H^* values were determined nevertheless was corrected by these factors before data reduction. Additionally, the fact that the correction factors turned out to be quite small, i.e., the decomposition of HNO₂ constitutes only a minor pathway for the removal of the aqueous-phase N(III) compared to the physical purging, indicates that the employment of values of k_5 , k_{-5} , and k_6 estimated for other temperatures that contain somewhat large uncertainties does not give rise to substantial error.

Comparison with Literature Values. *Henry's Law Solubility.* The Henry's law constant of HNO₂ corresponding to 25 °C is determined to be $49 \pm 3 \text{ M atm}^{-1}$ by interpolation. This value is between that reported by Abel and Neusser³⁹ as corrected by Wayne and Yost,⁴⁰ namely, 33 M atm^{-1} , and that calculated by Carta,⁴¹ namely, 59.2 M atm^{-1} . However, it is identical with the value calculated²⁰ from the standard free energies of formation for HNO₂(g) and HNO₂(aq) given by NBS 270-3.⁴³ This agreement lends support to the values of the solubilities of NO₂, N₂O₃, and N₂O₄ evaluated by Schwartz and White²⁰ using

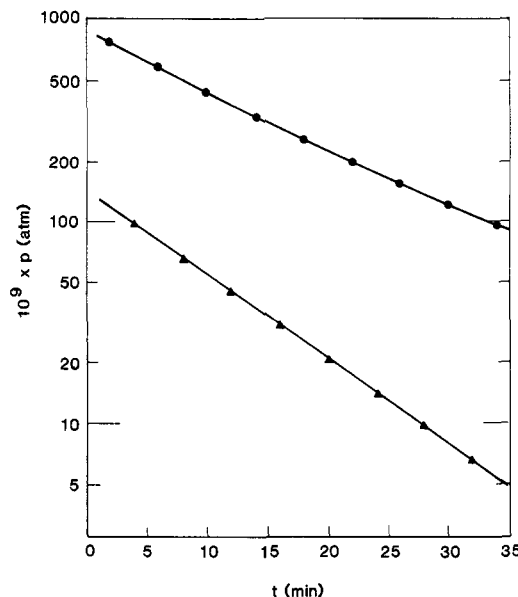


Figure 9. Time dependence of the partial pressures of nitrogen species purged from the gas-liquid reactor containing a $4.5 \times 10^{-5} \text{ M}$ HNO₂ solution. Individual points are experimental results, and the solid lines are calculated by using the rate constants reported in this study. Experimental conditions: $V_1 = 25.7 \text{ m}$, $F_g = 35 \text{ cm}^3 \text{ s}^{-1}$, pH 2.13, and temperature = 22.0 °C: (Δ) p_{NO} ; (\circ) p_{NO_y} = sum of NO, NO₂, and HNO₂.

thermochemical cycles involving the solution process of HNO₂.

Although the value of $\Delta G^{\circ}_{\text{sol}}$ of nitrous acid dissolution corresponding to 25 °C calculated by using $\Delta G^{\circ}(22^{\circ}\text{C}) = -2.40 \text{ kcal mol}^{-1}$ and $\Delta H^{\circ}_{\text{sol}} = -9.7 \text{ kcal mol}^{-1}$, both determined in this work, namely, $-2.33 \text{ kcal mol}^{-1}$, is identical with the value given by NBS 270-3,⁴³ it is significantly different from the value given in later reports,⁴⁴ $-1.1 \text{ kcal mol}^{-1}$. Additionally, the value of $\Delta S^{\circ}_{\text{sol}}$ determined in this work also agrees with the value ($-24.2 \text{ cal mol}^{-1} \text{ K}^{-1}$) reported in NBS publication 270-3⁴³ but not with the value ($-28.3 \text{ cal mol}^{-1} \text{ K}^{-1}$) in the later NBS publication 270-8.⁴⁴ The preference of the earlier thermodynamic value for $\Delta G^{\circ}_{\text{sol}}$ over the later value has also been pointed out by Ram and Stanbury in their recent study of the redox reactions of hexachloroiridate in nitrous acid solution.⁵² It should be mentioned that the value of $\Delta H^{\circ}_{\text{sol}}$ determined in this work agrees within the error limits with the value of $-9.5 \text{ kcal mol}^{-1}$ reported in both tabulations.

Reaction Kinetics. A comprehensive review of the rate constants of aqueous-phase reactions involving nitrogen oxides has been given by Schwartz and White.¹⁹ The value recommended in that work for k_5 at 25 °C is $5.6 \text{ M}^{-1} \text{ s}^{-1}$, representing the average of the isotope-exchange study by Bunton et al. ($5.8 \text{ M}^{-1} \text{ s}^{-1}$)⁵³ and the diazotization study by Hughes and Ridd, as well as the nitrosation study by Kalatzis and Ridd ($5.3 \text{ M}^{-1} \text{ s}^{-1}$, calculated from the rate constant determined at 0 °C).^{54,55} Although the value determined in this study, $13.4 \text{ M}^{-1} \text{ s}^{-1}$ at 22 °C, is greater than these values by more than a factor of 2, it is nonetheless in close agreement with the value $14 \text{ M}^{-1} \text{ s}^{-1}$ determined from the study of $\text{S}_2\text{O}_3^{2-}$ reaction with HNO₂ by Garley and Stedman⁵⁶ and $10\text{--}25 \text{ M}^{-1} \text{ s}^{-1}$, at 25 °C, from the study of hexachloroiridate redox couple in HNO₂ solution by Ram and Stanbury.⁵²

The value recommended by Schwartz and White¹⁹ for k_{-5} at 25 °C is $3 \times 10^7 \text{ M}^{-1} \text{ s}^{-1}$, with a lower bound of 1×10^7 and an upper bound of 1×10^8 , and for k_6 is $7 \times 10^7 \text{ M}^{-1} \text{ s}^{-1}$, with 3.5×10^7 and 1×10^8 as the lower and upper bounds, respectively. These values were derived from the direct kinetic studies of flash photolysis and pulse radiolysis by Grätzel et al.,²⁸ by Treinin and

(52) Ram, M. S.; Stanbury, D. M. *Inorg. Chem.* **1985**, *24*, 2954.

(53) Bunton, C. A.; Llewellyn, D. R.; Stedman, G. *J. Chem. Soc.* **1959**, 568.

(54) Hughes, E. D.; Ridd, J. H. *J. Chem. Soc.* **1958**, 70.

(55) Kalatzis, E.; Ridd, J. H. *J. Chem. Soc. B* **1966**, 529.

(56) Garley, M. S.; Stedman, G. *J. Inorg. Nucl. Chem.* **1981**, *43*, 2863.

Hayon,²⁹ and by a number of indirect studies of the absorption rate of NO_x species.³⁰⁻³⁶ The values of k_{-5} obtained in this study, $1.6 \times 10^8 \text{ M}^{-1} \text{ s}^{-1}$ at 22 °C, is greater than the upper limit value recommended by Schwartz and White, but it agrees well with the value, $1.75 \times 10^8 \text{ M}^{-1} \text{ s}^{-1}$, reported by Ram and Stanbury.⁵² The value of k_6 determined in this study, namely, $(8.4 \pm 1.5) \times 10^7 \text{ M}^{-1} \text{ s}^{-1}$, agrees reasonably well with that determined previously by this laboratory,³⁶ $(1.0 \pm 0.1) \times 10^8 \text{ M}^{-1} \text{ s}^{-1}$, and that recommended by Schwartz and White,¹⁹ $7 \times 10^7 \text{ M}^{-1} \text{ s}^{-1}$.

Implications for Atmospheric Chemistry. Cloud Chemistry. The concentration of N(III) in atmospheric water in equilibrium with gaseous HNO₂ is given by

$$[\text{N(III)}]_{\text{eq}} = H^* p_{\text{HNO}_2} = H_{\text{HNO}_2} (1 + K_a / [\text{H}^+]) p_{\text{HNO}_2} \quad (26)$$

For a typical cloudwater pH of 4 and an upper limit of 10 ppb⁴ for p_{HNO_2} , together with the Henry's law coefficient and the dissociation constant of HNO₂ determined in this work, $[\text{N(III)}]_{\text{eq}}$ at 25 °C is estimated to be $\leq 4 \times 10^{-6} \text{ M}$. This concentration of HNO₂ by itself is not expected to lead to any important contribution to cloudwater acidification. The production of NO, NO₂, and NO₃⁻ from the decomposition of HNO₂ calculated for the same atmospheric conditions are also found to be insignificant.

In the case of reactions leading to the oxidation of nitrous acid, i.e.



where Ox represents an oxidant, the reaction will be important only if the condition rate = $d[\text{NO}_3^-]/dt = k_{27}[\text{Ox}][\text{N(III)}] \geq 3 \times 10^{-6} \text{ M h}^{-1}$ is satisfied. It may be noted that the choice of $3 \times 10^{-6} \text{ M h}^{-1}$ is somewhat arbitrary. Again, for pH 4 and $p_{\text{HNO}_2} \leq 10 \text{ ppb}$, $k_{27}[\text{Ox}]$ must be greater than 0.75 s^{-1} for the reaction to be significant. By use of this criterion, the H₂O₂-N(III) reaction is judged unimportant for $[\text{H}_2\text{O}_2] \leq 3 \times 10^{-5} \text{ M}$.⁵¹ On the other hand, the O₃-N(III) reaction may be significant for $p_{\text{O}_3} \geq 20 \text{ ppb}$.⁵⁷

Atmospheric Sources of HNO₂. The potential importance of aqueous-phase reactions of nitrogen precursors to produce N(III) as sources of gas-phase nitrous acid can also be examined in light of the data obtained in this work. Since the Henry's law solubility of HNO₂ is rather limited, the material distribution of N(III) at equilibrium between the gas and liquid phase expressed as a ratio, i.e.

$$R_D = 1/H^*RTL \quad (28)$$

where L represents the liquid water concentration of a space volume, in units of m³/m³, is found to be smaller than 0.01 at a typical cloudwater pH of 4. Namely, any N(III) produced in aqueous droplets is nearly quantitatively released into the gas phase at equilibrium. Since cloudwater droplets are small, the rate of mass transport between the gas and liquid phases in clouds is believed to be much faster than the rates of accompanying chemical reactions and therefore is established instantaneously.⁵⁸ By assuming that a gas-phase HNO₂ buildup rate of 1 ppb h⁻¹ constitutes a rate at which the gas-phase production becomes important, the corresponding aqueous-phase rate of N(III) production for $L = 1 \times 10^{-6}$ should be $R^{(a)} = k^{(1)}[s] = 1.2 \times 10^{-8} \text{ M s}^{-1}$, where $k^{(1)}$ is the effective first-order rate constant and $[s]$ the aqueous concentration of the nitrogen(III) precursor. With

this criterion, the hydrolysis of some of the important atmospheric nitrogen species can be examined for their importance as an aqueous-phase nitrous acid precursor. For instance, peroxyacetyl nitrate (CH₃C(O)O₂NO₂, PAN), for which $H = 3.6 \text{ M atm}^{-1}$ and $k^{(1)} \cong 2 \times 10^{-4} \text{ s}^{-1}$, is^{59,60} judged unimportant as a precursor of HNO₂ at a typical atmospheric concentration of 1 ppb. On the other hand, the hydrolysis of peroxyntitric acid (HO₂NO₂, PNA), which has an effective Henry's law solubility of $\geq 2 \times 10^4 \text{ M atm}^{-1}$,⁶¹ may contribute significantly to HNO₂ production depending on its atmospheric concentration. Since the value of $k^{(1)}$ determined for the hydrolysis of PNA is $\sim 1 \times 10^{-2} \text{ s}^{-1}$ at pH 4,⁶¹ the gas-phase concentration of PNA must be present at a level comparable to or greater than $6 \times 10^{-11} \text{ atm}$ for the PNA pathway to be important.

Conclusion

The Henry's law solubility of nitrous acid in water and the kinetics of the reversible aqueous-phase decomposition of this species to NO and NO₂ and the subsequent disproportionation of NO₂ were determined by monitoring the gas-phase concentrations of these species as a function of time as purged from a bubbler-type gas-liquid reactor of known gas-liquid mass-transfer characteristics. Real-time measurement of the concentrations of these nitrogen oxides and oxyacid in the effluent gas, which were present in the sub-parts-per-billion range as being constrained by the present chemical and physical systems, was achieved by using a high-sensitivity ozone-chemiluminescence NO_x detector. The Henry's law coefficient of HNO₂ was determined to be $49 \pm 3 \text{ M atm}^{-1}$ at 25 °C. The standard heat of solution of HNO₂ ($\Delta H^\circ_{\text{sol}}$) determined for the temperature range 0-30 °C is $-9.7 \text{ kcal mol}^{-1}$. Although this value agrees well with that recommended by NBS, the value of $\Delta G^\circ_{\text{sol}}$ obtained in this work, i.e., $-2.3 \text{ kcal mol}^{-1}$ at 25 °C, is at variance with the value given in current NBS tables but is identical with the value recommended in earlier NBS tables. The acid dissociation constant of HNO₂ corrected to zero ionic strength was determined to be $5.3 \times 10^{-4} \text{ M}$ at 25.0 °C, in good agreement with literature values. The rate constants of the forward and reverse reactions of the reversible nitrous acid decomposition as defined in this work were determined to be $13.4 \pm 1.0 \text{ M}^{-1} \text{ s}^{-1}$ and $(1.58 \pm 0.13) \times 10^8 \text{ M}^{-1} \text{ s}^{-1}$, respectively. The rate constant of NO₂ disproportionation was determined to be $(8.4 \pm 1.5) \times 10^7 \text{ M}^{-1} \text{ s}^{-1}$. All the rate constants are reported for $22.0 \pm 0.1 \text{ °C}$. An argument is presented, using the information obtained in this work, that nitrous acid contributes insignificantly to the acidity of cloudwater or rainwater. However, it remains plausible that gas-phase nitrous acid observed in ambient air can result from aqueous-phase reactions of nitrogen precursors that produce N(III) followed by rapid mass transfer between the liquid and gas phases.

Acknowledgment. We acknowledge Drs. L. Newman and S. E. Schwartz for their encouragement and helpful discussions. This research was supported by the National Acid Precipitation Assessment Program through the PRECP Project and was performed under the auspices of the United States Department of Energy under Contract No. DE-AC02-76CH00016.

Registry No. NO₂, 10102-44-0; HNO₂, 7782-77-6.

(59) Holdren, M. W.; Spicer, C. W. *Atmos. Environ.* **1984**, *18*, 1171.

(60) Lee, Y.-N. In *Proceedings of Conference on Gas-Liquid Chemistry of Natural Waters*; Brookhaven National Laboratory: Upton, NY, 1984; Paper No. 20.

(61) Park, J.-Y.; Lee, Y.-N. Presented at the 193rd ACS National Meeting, Denver, April, 1987. Division of Physical Chemistry, Paper No. 67A.

(57) Damschen, D. E.; Martin, L. R. *Atmos. Environ.* **1983**, *17*, 2005.

(58) Schwartz, S. E. In *Chemistry of Multiphase Atmospheric Systems*; Jaeschke, W., Ed.; NATO ASI Series, Springer-Verlag: Berlin, 1986; Vol. G6, pp 415-471.